5th SASTech
Iran |Mashhad
May 12 - 17 | 2011
5th Symposium on Advances in Science & Technology

# Facile synthesis of $WS_2$ inorganic fullerene-like nanomaterials from $WS_2$ amorphous nanoparticles

S.Salar Meshkat[1]*, H.R.Gholami[1]

[1]Address: Iran, Urmia, Urmia University of Technology, Chemical Engineering Facaulty

E-mail:s.meshkat@che.uut.ac.ir

Paper Reference Number : 0104-701

Name of the Presenter: S.Salar Meshkat

**Abstract**

The amorphous $WS_2$ nanoparticles have been synthesized by a simple oxidation-reduction reaction in an aqueous solution. A series of products with different morphologies, such as $WS_2$ nano spheres, inorganic fullerene-like nanospheres, nanorods and W bended rods, can be obtained by annealing the amorphous $WS_2$ nanoparticles under $N_2$ atmosphere under 400-1200 $^0$C. These products have been characterized by X-ray diffraction, field emission scanning electronic microscopy, transmission electron microscopy and high-resolution transmission electron microscopy in detail. The possible transformation mechanism for the structure has been discussed based on the experimental results. In addition, the optical properties of IF-$WS_2$ have also been performed by UV-vis absorption spectroscopy.

**Keywords**: Fullerene, Nanostructures, Chemical synthesis, X-ray diffraction, Crystal structure

## 1.Introduction

Since the discovery of C60 molecule and carbon nanotubes, intense interests have been aroused to synthesize inorganic materials with fullerene-like (IF) structures and nanotubes from different inorganic compounds [1,2 .[ During the past years, the synthesis of transition metal dichalcognides $MX_2$ (M = W, Mo; X = S, Se) with IF structure and nanotubes [3-5] has opened a challenging new field in solid state physics, chemistry and materials science with a wide range of possible applications, such as electrochemical hydrogen storage [6], cathode material for rechargeable lithium batteries and solar cell materials [7,8], electric transport [9], useful solid lubricant [10], sulfur removal catalyst [11] and an intercalation host [12]. Since the IF-$MX_2$ initially synthesized by Tenne and co-workers, a large variety of forms ranging from nanoparticles, nanotubes, nanosheets,

nanofibers, and nanobelts to fullerenes have been obtained [13-15]. In order to elucidate the growth mechanism and to produce the materials for large-scale commercial applications, many synthetic routes have been developed from their first formation from respective trioxides in $H_2S$ and $N_2/H_2$ atmosphere by gas solid or gas-gas reactions, such as electron-beam irradiation activation and arc discharge [16,17], hydrothermal or solvothermal synthesis [18,19], sonochemical process [20], template synthesis [21], atmospheric pressure chemical vapor deposition [22,23] and electrochemical/chemical synthesis [24]. An economical and effective method for large-scale synthesis of high quality IF-$MoS_2$ and $WS_2$ is always a challenge for the scientists. Here we report a simple and low-cost route to synthesize the amorphous $WS_2$ nanoparticles by oxidation-reduction reaction in aqueous solution. A series of products with different morphologies, such as $WS_2$ nanospheres, IF-nanospheres and nanorods can be obtained by annealing the amorphous $WS_2$ in $N_2$ atmosphere. The interest in $WS_2$ nanostructure is considered a focal at present. In the paper, we investigate the transformation of nanostructure of $WS_2$ annealed at different temperatures in detail in order to evaluate the thermal stability of IF structure and to control the morphology of samples. The synthesis route may offer an opportunity for fundamental studies and technological applications.

## 2. Experimental

### 1.2 Preparation

The preparation of amorphous $WS_2$ nanoparticles was carried out by adding $(NH_4)_6W_7O_{24}$ $4H_2O$ (AR, 0.88 g) and $Na_2S$ $9H_2O$ (AR, 2.64 g) to 100 mL HCl solution (0.8 mol $L^{-1}$) in a 250 mL round-bottom flask with vigorous stirring. Heated at 80 8C for 0.5 h, $NH_2OH$ HCl (AR, 0.7 g) was added all at once then with vigorous stirring for 1 h . The black powder finally was obtained by centrifugal separation and washed with deionized water for several times to remove the residue of the reactants, then dried in the air to obtain the final product of $WS_2$ powder .The $WS_2$ powder was annealed in a sealed muffle under $N_2$ atmosphere (0.5-0.8 105Pa) for 2 h at different temperatures (400-1200 8C). The detailed experimental equipment is described in the reference [25].

### 2.2 Characterizations

The phase-structures and morphology of the as-prepared samples were characterized by X-ray diffraction (XRD ,D/max-rA) employing Cu Ka radiation, field emission scanning electronic microscopy (FESEM, JSM-6700F ,(transmission electron microscopy (TEM, H-800EM), and high-resolution transmission electron microscopy (HRTEM ,JEM-3010). Optical characterization of IF-MoS2 was performed by UV-vis absorption spectroscopy (UV-vis).

3.Results and discussion

Fig. 1 shows the XRD patterns of the final products synthesized at different annealing temperatures. Fig. 1(a) indicates that the X-ray spectrum is confined to a wide and weak (0 0 2) peak of the amorphous $WS_2$ synthesized by the oxidation-reduction described by the following reaction:

1) $(NH_4)_2WO_4 + 4Na_2S + 8HCl \rightarrow (NH_4)_2WS_4 + 8NaCl + 4H_2O$
2) $(NH_4)_2WS_4 + 2NH_2OH + HCl \rightarrow WS_2 + N_2 + 2NH_4Cl + 2H_2O + 2H_2S$

With the temperature increasing from 400 to 900 8C, more peaks appeared and became sharper meanwhile the peak intensities increased rapidly. The above results indicated that the morphology became more integrated and 2H-WS2 with characteristic peaks of (0 0 2), (0 0 4), (1 0 0), (1 0 2), (1

0 3), (1 0 4), (1 0 5), (1 1 0), (1 1 2), (1 1 6), (2 0 0 )appeared at the annealing temperature of 900 $^0$C (indexing JCPDS file No. 87-2416 .(But the (0 0 2) peaks during the thermal process have no distinct shift comparing with the corresponding value (about %2 reported by Tenne et al. With the temperature increasing to 1000 $^0$C, $W_2S_3$ appeared and at 1100 8C $W_2S_3$ mostly transformed into Mo. Pure body-centered cubic metal Mo is obtained at 1200 $^0$C with characteristic peaks of (110) and (2 2 0). Thus, controlling suitable temperature is a key factor to obtain samples with different morphologies .

Fig. 2 shows the morphologies of the $WS_2$, $W_2S_3$ and W obtained at different annealing temperatures. It was obvious that the morphology and the size of the samples were distinctly different during the thermal treatment. From Fig. 2(a) it could be seen that the sample annealed at 400 8C were mainly small nanoparticles with the diameter about 30 nm. While during the thermal treatment at 800 8C, a majority of nanoparticles grew along c axes then $WS_2$ nanorods can be obtained. Indicated from XRD and FESEM images, sheet $W_2S_3$ and W bended nanorods were obtained at 1000 $^0$C and 1200 $^0$C, respectively .

The TEM images in Fig. 3 revealed the dramatic changes in the overall appearance of the samples following the heat treatments. At lower annealing temperature, such as 400 $^0$C, near monodisperse $WS_2$ nanospheres can be obtained and the majority is with the diameter of 20-70 nm (Fig. 3(a)). Driven by the thermal energy, the IF shell come into being due to the sulfur bonds breaking for recrystallization of amorphous $WS_2$ and the elimination of unsaturated bonds at the edge of $WS_2$ (Fig. 3(b)). With the temperature increased to 700 $^0$C, elliptical polyhedron of $WS_2$ with nested core is produced with the port connected each other (Fig. 3(c)). And the rod-like $WS_2$ is obtained at 800 0 $^0$C with 30 nm in diameters and 100-200 nm in length (Fig. 3(d)). The electron diffraction pattern of Fig. 3(g) indicates the $WS_2$ with (0 0 2), (1 0 0), (1 0 3) and (1 1 0) planes. With the temperature increased to 1000 $^0$C, clubbed $W_2S_3$ with core-shell structure appears (Fig. 3(e)). The selected area electron diffraction of Fig. 3(h) shows the Mo2S3 single crystal shell. At elevated temperature of 1200 $^0$C rod-like W is the main phase because of the decomposition of $WS_2$ (Fig. 3(f)). The floc on Mo surface may be the amorphous sulfide formed during the descent of temperature. Thus, the annealing temperature should be controlled at 500-700 $^0$C in order to get IF structure .

More details for $WS_2$ at elevated temperatures are illustrated by HRTEM studies in Fig. 4. The series of images indicated the transformation in IF structures. The morphologies indicate that at the annealing temperatures of 600 $^0$C the nested and closed structure with several layers of the particle is relatively integrated but the defect is obvious at the corner (Fig. 4(b)). However, with the annealing temperature increased to 900 $^0$C, the closed cage is broken and a side in IF structure disappears (Fig. 4(c)). The typical morphology of irregular strip is showed in Fig. 4(d) with fringe distance of 0.62 nm and 5 nm wide under the same thermal situation. Furthermore, bended rod of $W_2S_3$ and open-ended W rod with core-shell structure was observed at the elevated temperature of 1000 $^0$C and 1100 $^0$C (Fig. 4(e and f)), respectively. And the shell indicates the fringe thickness of 0.21 nm for W (1 1 0) lattice (Fig. 4f) .The growth mechanism for IF structure can be described as follows: According to XRD and energy-dispersive spectroscopy results, the initially obtained nanoparticles are amorphous and the molar ratio of sulfur to molybdenum is about 2.2:1 (the EDS spectra are not shown here). During the thermal treatment, the rich sulfur bonds broke first for recrystallization of $WS_2$. Driven by thermal kinetics, the IF nanoparticles were obtained by eliminating the unsaturated bonds to form a closed structure. While, the IF nanostructures in our experiment have many defects especially at the corner and periphery. The defects may help to release some strain in the folded layers, so the d(0 0 2 ) have no obvious change and the (0 0 2) peaks in XRD do not show distinct shifts. At elevated temperature, the closed structures become unstable and the layers brake, thus the nanorods of $WS_2$ are

formed. Due to the decomposition of $WS_2$ by controlling the temperature, a special phase of $W/WS_2$ (Fig. 4(f)) and an intergradation of $W_2S_3$) Fig. 2(c)) come into being. Because the disconnection could easily occur at the corner, the metal Mo with branches can be obtained. The unique morphology for W may be applied as accession to enhance mechanical performance and offer catalytic applications .Optical characterization of IF-$WS_2$ was performed by UV-vis absorption spectroscopy at room temperature .Fig. 5 shows the UV-vis absorption spectra of IF-$WS_2$ suspension. The spectral data show stronger absorption in the blue region and weaker absorption in the red region. It displayed a strong and broad line from 290 to 400 nm with a maximum centered at about 340 nm and weaker absorbance during 500-670 nm (in Fig. 5(b and c)). It is known that the direct band gap of $WS_2$ is located in the visible (ca. 700 nm) and two further more bands occur at ca. 500 nm and 350 nm both associated with the direct transitions from the valence band to the conduction band [26]. Fig. 5 matched well with the above description, although the band threshold for the less energetic direct transition is slightly blue shifted from the typical wavelength of 700 nm. This may be because that the $WS_2$ nanoparticles used in the test have bigger dimensions than 4.5 nm $WS_2$ clusters in reference [26] and the dimensions should be in the limit for which quantum size effects are expected. In addition, the absorbance became stronger with annealing temperature increased. This may be due to the size of the sample and the IF layers increased .

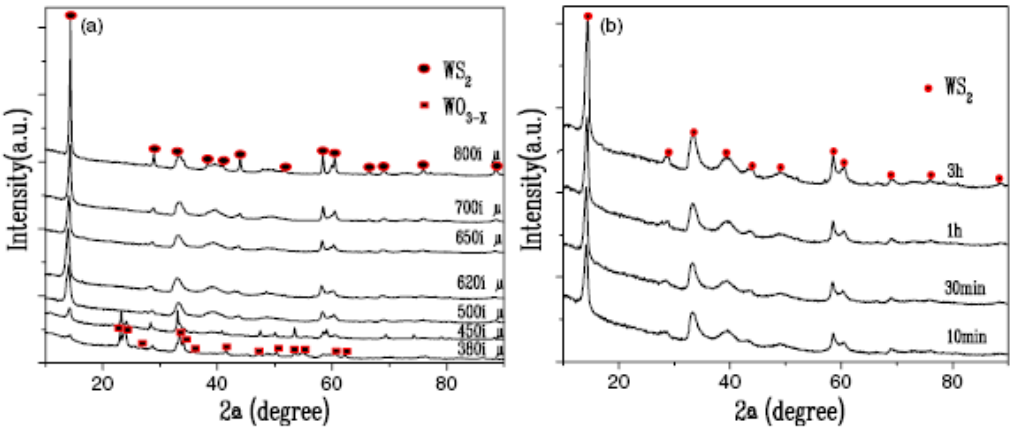


Fig. 1. XRD patterns of (a) as-synthesized $WS_2$ nanoparticles without being annealed; the samples annealed at different temperatures: (b) 400 $^0$C ;(c) 500 $^0$C; (d) 600 $^0$C; (e) 900 $^0$C; (f) 1000 $^0$C; (g) 1100 $^0$C; (h) 1200 $^0$C.

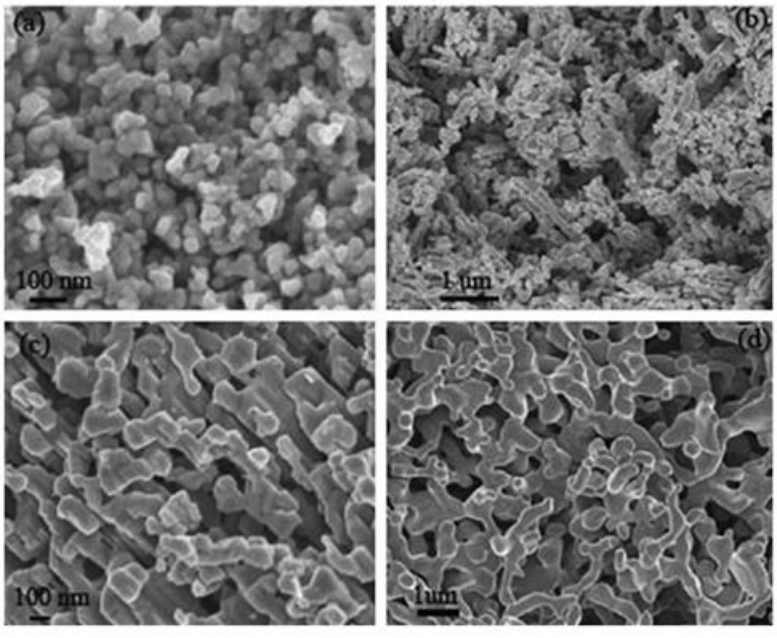

Fig. 2. SEM images for amorphous $WS_2$ annealed at different temperatures: (a) 400 $^0$C, (b) 800 $^0$C, (c) 1000 $^0$C, and (d) 1200 $^0$C.

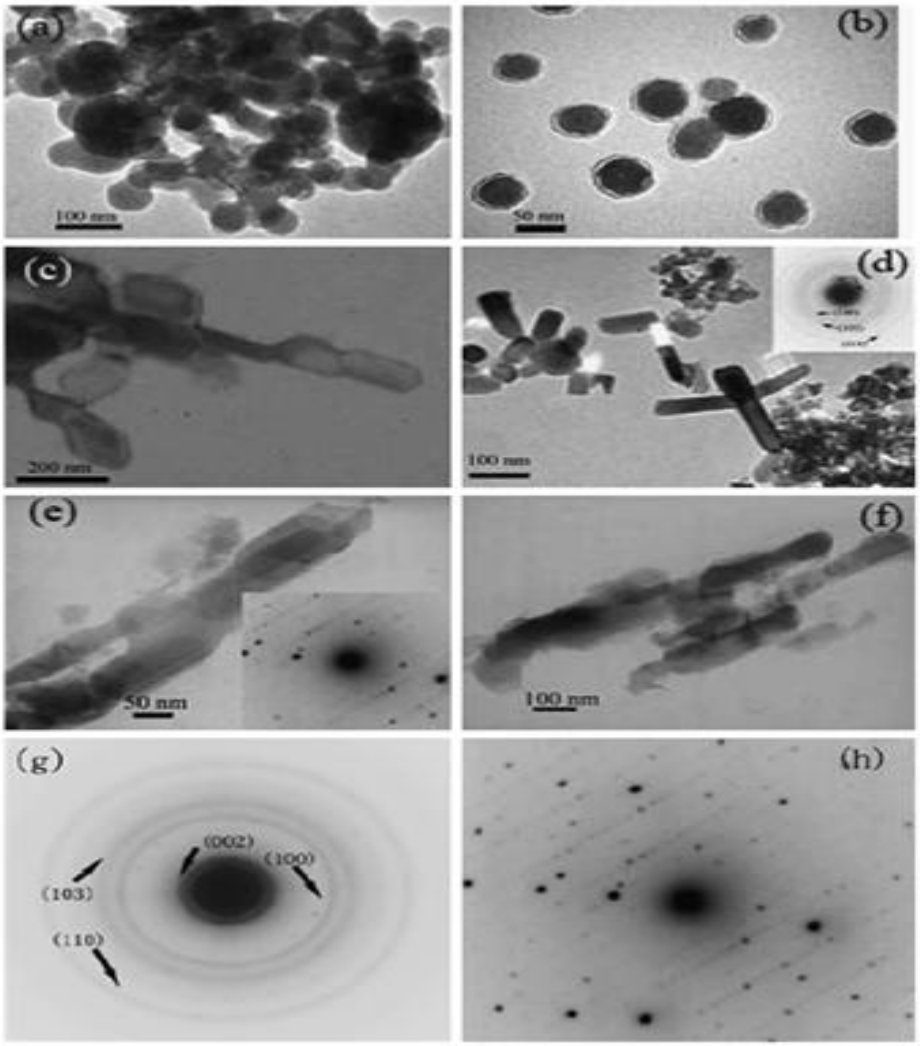


Fig. 3. TEM images for amorphous $WS_2$ annealed at different temperatures: (a) 400 $^0$C, (b) 500 $^0$C, (c) 700 $^0$C, (d) 800 $^0$C, (e) 1000 $^0$C, (f) 1200$^0$C, and (g and h) electron diffraction patterns for the samples of (d) and (e).

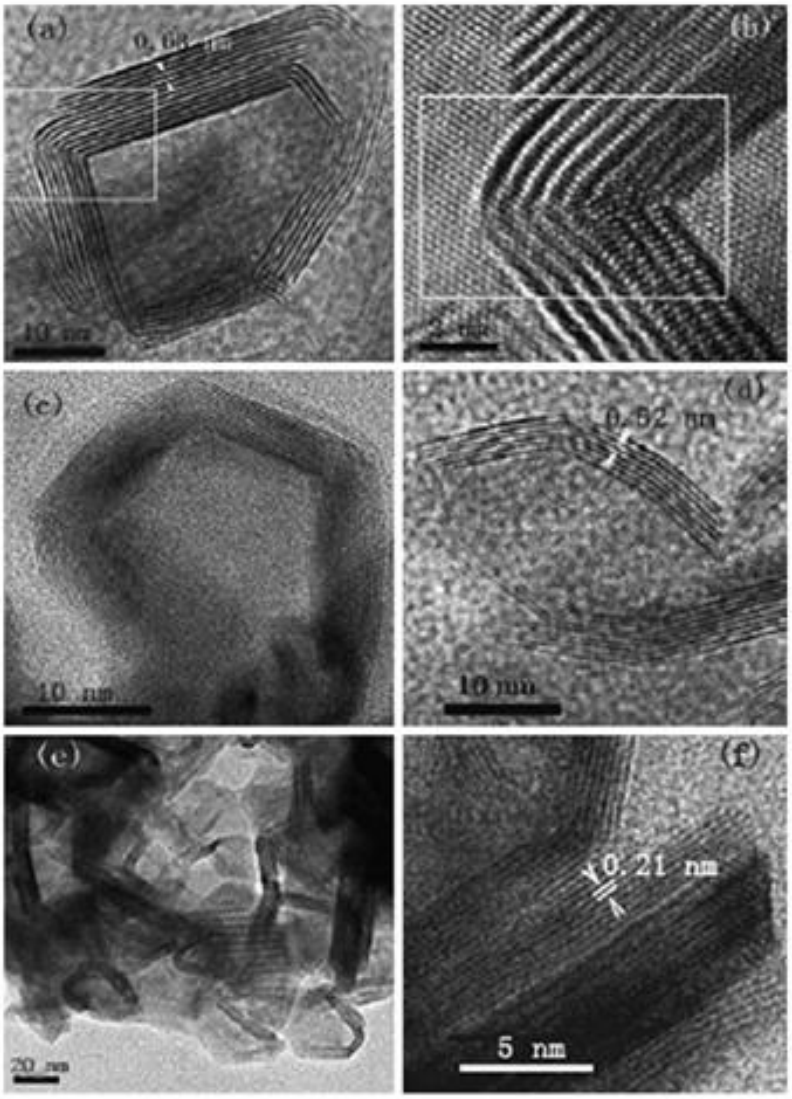


Fig. 4. HRTEM images of the annealed amorphous $WS_2$ at higher temperatures (a) annealed at 600 $^0$C with $WS_2$ d(0 0 2) of 0.63 nm; (b) enlarged image of (a) in the rectangle and indicated the obvious effects at the corner in IF structure; (c) annealed at 900 $^0$C; (d) annealed at 900 $^0$C with highmagnification and with $WS_2$ d(0 0 2) of 0.62 nm; (e) annealed at 1000 $^0$C; (f) 1100 $^0$C, W nanorod with core-shell structure and the shell show W (110) lattice of about 0.21 nm.

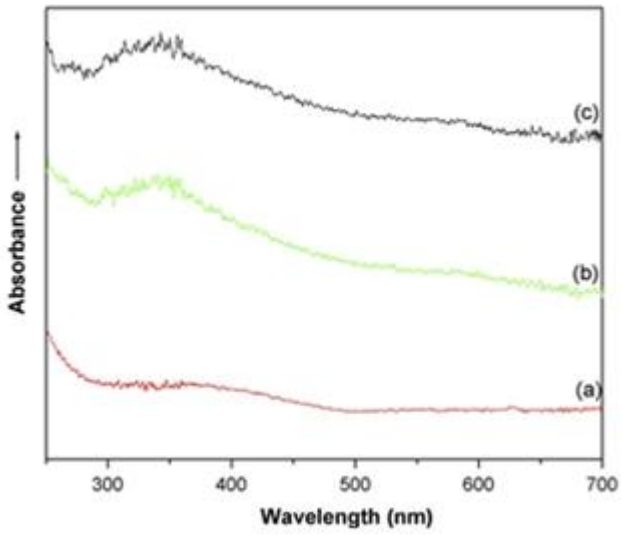


Fig. 5. UV-vis absorption spectroscopy of the IF nanospheres obtained at (a) 500 $^0$C; (b) 600 $^0$C; (c) 700 $^0$C.

## 4. Conclusions

Amorphous $WS_2$ nanospheres were obtained by a one-step oxidation-reduction reaction in solution. Because of the rich sulfur bonds broken and the unsaturated bonds eliminated by controlling the annealing temperatures, a series of products have been synthesized, $WS_2$ nanospheres with diameter of 20-70 nm, IF-nanospheres with diameter of around 20 nm and single crystal of W rods with length from hundreds of nanometers to several microns. The IF structure with many defects at the corner and periphery caused the break driven by the thermal kinetics. This may be the main reason for the formation of the bended nanorods. The IF $WS_2$ nanospheres obtained by us have a relatively strong and broad visible absorption spectroscopy from 290 to 400 nm and a weak absorption at the region of 500 - 670 nm with a slightly blue shift. The present route is easy to control over all the reaction processes and the simple synthesis with low-cost may offer an alternative rout to synthesize the transition metal dichalcognides with IF structure and transition metal nanorods .

References

[1] H.W. Kroto, J.R. Heath, S.C. O'Brien, R.F. Curl, R.E. Smalley, Nature 318 (1985) 162.

[2] S. Iijima, Nature 354 (1991) 56 .

[3] R. Tenne, L. Margulis, M. Genut, G. Hodes, Nature 360 (1992) 444 .

[4] L. Margulis, G. Salitra, R. Tenne, M. Talianker, Nature 365 (1993) 113 .

[5] M. Hershfinkel, L.A. Gheber, V. Volterra, J.L. Hutchison, L. Margulis, R. Tenne, J. Am. Chem. Soc. 116 (1994) 1914.

[6] J. Chen, N. Kuriyama, H.T. Yuan, H.T. Takeshita, T. Sakai, J. Am. Chem. Soc. 123 (2001) 11813 .

[7] N. Imanishi, K. Kanamura, Z. Takehara, J. Electrochem. Soc. 139 (1992) 2082 .

[8] M. Thomalla, H. Tributsch, J. Phys. Chem. B 110 (2006) 12167 .

[9] F. Kopnov, G. Leitus, A. Yoffe, I. Feldman, A.M. Panich, R. Tenne, Phys. Stat. Sol. 243 (2006) 3290.

[10] L. Rapoport, N. Fleischer, R. Tenne, Adv. Mater. 15 (2003) 651 .

[11] S.E. Skrabalak, K.S. Suslick, J. Am. Chem. Soc. 127 (2005) 9990 .

[12] E. Aharon, A. Albo, M. Kalina, L. Frey Gitti, Adv. Funct. Mater. 16 (2006) 980.

[13] M. Nath, A. Govindaraj, C.N.R. Rao, Adv. Mater. 13 (2001) 283 .

[14] C.M. Zelenski, P.K. Dorhout, J. Am. Chem. Soc. 120 (1998) 743 .

[15] L. Rapoport, Y. Bibik, Y. Feldman, M. Homyonfer, S.R. Cohen, R. Tenne, Nature 387 (1997) 791 .

[16] M. Jose-Yacaman, H. Lorez, P. Santiago, D.H. Galvan, I.L. Garzon, A. Reyes, Appl. Phys. Lett. 69 (1996) 1065.

[17] P.A. Parilla, A.C. Dillon, K.M. Jones, G. Riker, D.L. Schulz, D.S. Ginley, M.J. Heben, Nature 397 (1999) 114.

[18] Y. Tian, Y. He, Y.F. Zhu, Chem. Lett. 8 (2003) 268 .

[19] D. Duphil, S. Bastide, C. Levy-Clèment, J. Mater. Chem. 12 (2002) 2430 .

[20] I. Uzcanga, I. Bezverkhyy, P. Afanasiev, C. Scott, M. Vrinat, Chem. Mater. 17 (2005) 3575 .

[21] L.X. Chang, H.B. Yang, J.X. Li, W.Y. Fu, Y.H. Du, K. Du, Q.Y. Yu, J. Xu, M.H. Li, Nanotechnology 17 (2006) 3827.

[22] X.L. Li, J.P. Ge, Y.D. Li, Chem. Eur. J. 10 (2004) 6163 .

[23] J. Etzkorn, A.H. Therese, F. Rocker, N. Zink, U. Kolb, W. Tremel, Adv. Mater. 17 (2005) 2372.
[24] Q. Li, J.T. Newberg, E.C. Walter, J.C. Hemminger, R.M. Penner, Nano Lett. 4 (2004) 277 .

[25] H.B. Yang, S.K. Liu, J.X. Li, M.H. Li, G. Peng, G.T. Zou, Nanotechnology 17 (2006) 1512.

[26] J.P. Wilcoxon, P.P. Newcomer, G.A. Samara, J. Appl. Phys. 81 (1997) 7934.